Restoration of ultrasound images using spatially-variant kernel deconvolution

Mihai I. Florea* , Adrian Basarab†,
Denis Kouamé†, Sergiy A. Vorobyov*

* Department of Signal Processing and Acoustics, Aalto University, Espoo, Finland
†IRIT UMR CNRS 5505, University of Toulouse, Toulouse, France

April 20, 2018

ICASSP 2018, Calgary, Canada

Background

Existing ultrasound image formation models

- [1,2] 2D convolution between the tissue reflectivity function (TRF) and a fixed system point-spread function (PSF)
- [3] spatially varying kernel convolution
    - spatially varying kernel
    - constant reference kernel modulated by the exponential of a fixed discrete generator
    - overly restrictive
- [4] arbitrary linear model with dense matrix representation
    - reconstruction limited to medium size images

[1] C. Dalitz, R. Pohle-Frohlich, and T. Michalk, "Point spread functions and deconvolution of ultrasonic images," *IEEE Trans. Ultrason. Ferroelectr. Freq. Control*, vol. 62, no. 3, pp. 531–544, Mar. 2015.

[2] N. Zhao, A. Basarab, D. Kouamé, and J.-Y. Tourneret, "Joint segmentation and deconvolution of ultrasound images using a hierarchical Bayesian model based on generalized Gaussian priors," *IEEE Trans. Image Process.*, vol. 25, no. 8, pp. 3736–3750, 2016.

[3] O. V. Michailovich, "Non-stationary blind deconvolution of medical ultrasound scans," in *Proc. SPIE*, vol. 101391C, Mar. 2017.

[4] L. Roquette, M. M. J.-A. Simeoni, P. Hurley, and A. G. J. Besson, "On an analytical, spatially-varying, point-spread-function," in *2017 IEEE International Ultrasound Symposium (IUS)*, Sep. 2017, Washington D.C., USA.

Pulse-echo emission of focused waves

- the most widely used acquisition scheme in ultrasound imaging.
- sequential transmission of narrow focused beams
- each transmission centered at a lateral position
- laterally invariant kernels
- kernels become wider away from the focal depth
  - dynamic focusing in reception and time gain compensation cannot fully compensate
  - spatial resolution degradation away from focal depth
  - need for an axially-variant kernel model

Axially-variant kernel ultrasound imaging model

$$\mathbf{y} = \mathbf{HPx} + \mathbf{n},$$

- $\mathbf{x}$ - tissue reflectivity function (TRF) to be recovered
- $\mathbf{y}$ - observed radio-frequency (RF) image
- $\mathbf{n}$ - independent identically distributed (i.i.d.) additive noise
  - we assume white Gaussian but not essential
- Operator $\mathbf{P} : \mathbb{R}^{m_t \times n_t} \to \mathbb{R}^{m_p \times n_p}$ pads the TRF with a boundary of width n_r and height m_r.
  - simple Kronecker structure
  - can be stored in memory as a sparse matrix
- Operator $\mathbf{H} : \mathbb{R}^{m_p \times n_p} \to \mathbb{R}^{m_t \times n_t}$ performs the axially-variant kernel convolution

Notation: discrete convolution

Valid convolution $\mathscr{C}_1(\mathbf{k})\mathbf{a} \stackrel{\text{def}}{=} \mathbf{k} *_1 \mathbf{a}$

Full convolution $\mathscr{C}_2(\mathbf{k})\mathbf{a} \stackrel{\text{def}}{=} \mathbf{k} *_2 \mathbf{a}$

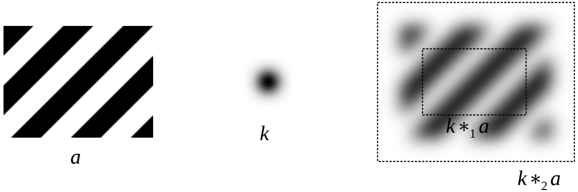

(a)

Figure : Convolving test image **a** with a Gaussian kernel **k**. The inner rectangle represents valid convolution whereas the outer marks full convolution; Here, black and white correspond to values of 1 and 0, respectively. Kernel **k** is displayed after min-max normalization.

Notation: auxiliary operators

Rotation operator (180°)	$\mathscr{R}(\mathbf{k})$
Full-width window operator	$\mathscr{W}_s(i_1, i_2)$
Zero padding operators	$\mathscr{Z}_s(i_1, i_2)$

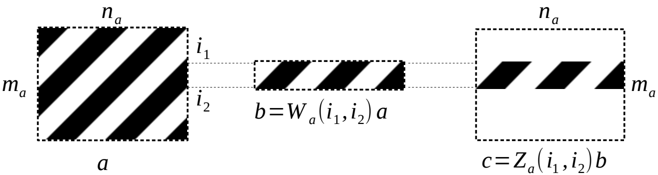

(b)

Figure : Applying the full-width window operator, followed by a full-width zero-padding operator on a test image **a**.

Axially varying convolution

Each *row* $i_h \in \{1, ..., m_t\}$ of the output image is obtained by the valid convolution between the kernel of that row $\mathbf{k}(i_h)$ and the corresponding patch in the input image $\mathscr{W}_p(i_h, i_h + 2m_r)\mathbf{x}$.

$$\mathbf{H} = \sum_{i_h=1}^{m_t} \mathscr{Z}_t(i_h, i_h)\mathscr{C}_1(\mathbf{k}(i_h))\mathscr{W}_p(i_h, i_h + 2m_r).$$

Need for adjoint of model operator

- Many deconvolution models use proximal splitting methods that optimize an objective containing a data fidelity term $\phi(\mathbf{HPx} - \mathbf{y})$.
- These methods employ at every iteration the gradient of the data fidelity term

$$\nabla(\phi(\mathbf{HPx} - \mathbf{y})) = \mathbf{P}^T \mathbf{H}^T (\nabla\phi)(\mathbf{HPx} - \mathbf{y}).$$

- We need computationally efficient expressions of $\mathbf{P}^T$ and $\mathbf{H}^T$

Efficient adjoint of model operator

Fundamental result on discrete convolution

Theorem

The adjoint of valid convolution is full convolution with the rotated kernel

$$(\mathscr{C}_1(\mathbf{k}))^T = \mathscr{C}_2(\mathscr{R}(\mathbf{k})).$$

Matrix-free expression for $\mathbf{H}^T$

$$\mathbf{H}^T = \sum_{i_h=1}^{m_t} \mathscr{Z}_p(i_h, i_h + 2m_r)\mathscr{C}_2(\mathscr{R}(\mathbf{k}(i_h)))\mathscr{W}_t(i_h, i_h).$$

$\mathbf{P}^T$ obtained using sparse matrix transposition

Ultrasound image deconvolution problem

Minimize the additive white Gaussian noise subject to elastic net regularization

$$\min_{\mathbf{x}\in\mathscr{D}_f} \frac{1}{2}\|\mathbf{HPx}-\mathbf{y}\|_2^2+\lambda_1\|\mathbf{x}\|_1+\frac{\lambda_2}{2}\|\mathbf{x}\|_2^2. \tag{1}$$

Objective F can be split into a quadratic function f and an elastic net regularizer Ψ

$$f(\mathbf{x})=\frac{1}{2}\|\mathbf{Ax}-\mathbf{y}\|_2^2, \quad \Psi(\mathbf{x})=\lambda_1\|\mathbf{x}\|_1+\frac{\lambda_2}{2}\|\mathbf{x}\|_2^2,$$

where $\mathbf{A} \overset{\text{def}}{=} \mathbf{HP}$.

- $\mathbf{A}$ is ill conditioned
- Ψ is not differentiable
- Lipschitz constant of $\nabla f(\mathbf{x})$ may be intractable to compute.

Optimization algorithm

The Accelerated Composite Gradient Method (ACGM)

- Applicable to all composite problems
- State-of-the-art convergence rate
  - For non-strongly convex objectives
    - Same asymptotic rate as FISTA of $O(1/k^2)$
    - Provably better constant
  - For strongly-convex objectives
    - Linear rate $O((1-\sqrt{q})^k)$
- Estimation of $\nabla f(\mathbf{x})$ Lipschitz constant
  - Automatic and dynamic at every iteration
  - Lipschitz constant does not have to exist globally
- Twice as fast for objectives of type $\tilde{f}(\mathbf{Ax}) + \Psi(\mathbf{x})$

ACGM (unoptimized)

Input: $\mathbf{x}_0,\ \lambda_1,\ \lambda_2,\ k_{max}$

$\mathbf{x}^{(-1)} = \mathbf{x}^{(0)}$

$L^{(0)} = \|\mathbf{HPx}^{(0)}\|_2^2 / \|\mathbf{x}^{(0)}\|_2^2$

$q^{(0)} = \frac{\lambda_2}{L^{(0)} + \lambda_2}$

$t^{(0)} = 0$

for $k = 0, ..., k_{max} - 1$ **do**

  $\alpha := 1 - q^{(k)} (t^{(k)})^2$

  $L^{(k+1)} := r_d L^{(k)}$

  loop

    $q^{(k+1)} := \frac{\lambda_2}{L^{(k+1)} + \lambda_2}$

    $t^{(k+1)} := \frac{1}{2} \left(\alpha + \sqrt{\alpha^2 + 4 \frac{L^{(k+1)} + \lambda_2}{L^{(k)} + \lambda_2} (t^{(k)})^2} \right)$

    $\beta := \frac{t^{(k)} - 1}{t^{(k+1)}} \frac{1 - q^{(k+1)} t^{(k+1)}}{1 - q^{(k+1)}}$

    $\mathbf{z}^{(k+1)} := \mathbf{x}^{(k)} + \beta (\mathbf{x}^{(k)} - \mathbf{x}^{(k-1)})$

    $\tau := 1 / L^{(k+1)}$

    $\mathbf{G} := \mathbf{P}^T \mathbf{H}^T (\mathbf{HPz}^{(k+1)} - \mathbf{y})$

    $\mathbf{x}^{(k+1)} := \frac{1}{1 + \tau\lambda_2} \mathscr{T}_{\tau\lambda_1} (\mathbf{z}^{(k+1)} - \tau \mathbf{G})$

    if $\|\mathbf{HPx}^{(k+1)} - \mathbf{HPz}^{(k+1)}\|_2^2 \leq L^{(k+1)} \|\mathbf{x}^{(k+1)} - \mathbf{z}^{(k+1)}\|_2^2$ **then**

      Break from loop

    else

      $L^{(k+1)} := r_u L^{(k+1)}$

    end if

  end loop

end for

Output: $\mathbf{x}^{(k_{max})}$

Reducing computational intensity of ACGM

At every iteration k, ACGM computes

- auxiliary point $\mathbf{z}^{(k+1)}$ by iterate extrapolation

$$\mathbf{z}^{(k+1)} = \mathbf{x}^{(k)} + \beta(\mathbf{x}^{(k)} - \mathbf{x}^{(k-1)})$$

- quatities $\mathbf{A}\mathbf{z}^{(k+1)}$ and $\mathbf{A}\mathbf{x}^{(k+1)}$ in $\nabla f(\mathbf{z}^{(k+1)})$ and line-search

Linearity of gradient and extrapolation presents opportunity

- cache all values

$$\tilde{\mathbf{x}}^{(i)} = \mathbf{A}\mathbf{x}^{(i)},\ i \in \{0, ..., k\}$$

- obtain without applying $\mathbf{A}$ the auxiliary point

$$\tilde{\mathbf{z}}^{(k+1)} \stackrel{\text{def}}{=} \mathbf{A}\mathbf{z}^{(k+1)} = \tilde{\mathbf{x}}^{(k)} + \beta(\tilde{\mathbf{x}}^{(k)} - \tilde{\mathbf{x}}^{(k-1)})$$

ACGM (optimized)

Input: $\mathbf{x}_0,\ \lambda_1,\ \lambda_2,\ k_{max}$
$\tilde{\mathbf{x}}^{(0)} := \mathbf{HPx}^{(0)}$,
$\mathbf{x}^{(-1)} = \mathbf{x}^{(0)}, \quad \tilde{\mathbf{x}}^{(-1)} = \tilde{\mathbf{x}}_0$
$L^{(0)} = \|\tilde{\mathbf{x}}^{(0)}\|_2^2 / \|\mathbf{x}^{(0)}\|_2^2$
$q^{(0)} = \frac{\lambda_2}{L^{(0)}+\lambda_2}$
$t^{(0)} = 0$
for $k = 0, \ldots, k_{max} - 1$ **do**
  $\alpha := 1 - q^{(k)} (t^{(k)})^2$
  $L^{(k+1)} := r_d L^{(k)}$
  loop
    $q^{(k+1)} := \frac{\lambda_2}{L^{(k+1)}+\lambda_2}$
    $t^{(k+1)} := \frac{1}{2}\left(\alpha + \sqrt{\alpha^2 + 4\frac{L^{(k+1)}+\lambda_2}{L^{(k)}+\lambda_2}(t^{(k)})^2}\right)$
    $\beta := \frac{t^{(k)}-1}{t^{(k+1)}} \frac{1-q^{(k+1)}t^{(k+1)}}{1-q^{(k+1)}}$
    $\mathbf{z}^{(k+1)} := \mathbf{x}^{(k)} + \beta(\mathbf{x}^{(k)} - \mathbf{x}^{(k-1)}), \quad \tilde{\mathbf{z}}^{(k+1)} := \tilde{\mathbf{x}}^{(k)} + \beta(\tilde{\mathbf{x}}^{(k)} - \tilde{\mathbf{x}}^{(k-1)})$
    $\tau := 1/L^{(k+1)}$
    $\mathbf{G} := \mathbf{P}^T \mathbf{H}^T (\tilde{\mathbf{z}}^{(k+1)} - \mathbf{y})$
    $\mathbf{x}^{(k+1)} := \frac{1}{1+\tau\lambda_2} \mathscr{T}_{\tau\lambda_1}(\mathbf{z}^{(k+1)} - \tau\mathbf{G}), \quad \tilde{\mathbf{x}}^{(k+1)} := \mathbf{HPx}^{(k+1)}$
    if $\|\tilde{\mathbf{x}}^{(k+1)} - \tilde{\mathbf{z}}^{(k+1)}\|_2^2 \leq L^{(k+1)} \|\mathbf{x}^{(k+1)} - \mathbf{z}^{(k+1)}\|_2^2$ **then**
      Break from loop
    else
      $L^{(k+1)} := r_u L^{(k+1)}$
    end if
  end loop
end for
Output: $\mathbf{x}^{(k_{max})}$

Simulation: forward model

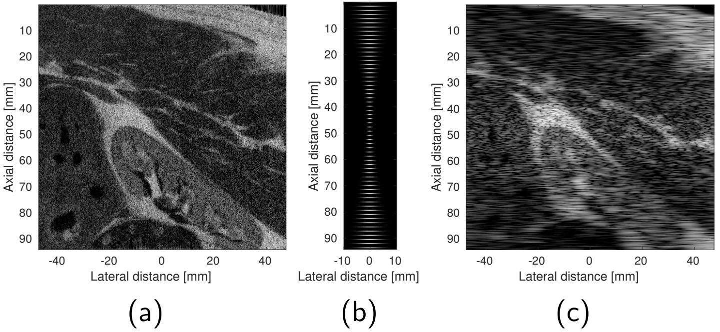

Figure : (a) Ground truth (in B-mode) of the tissue reflectivity function (TRF); (b) Demodulated kernels $\mathbf{k}(i_h)$ for twenty depths at regularly spaced intervals of 2 mm; (c) Observed B-mode image simulated following the proposed axially-variant convolution model;

Simulation: reconstruction

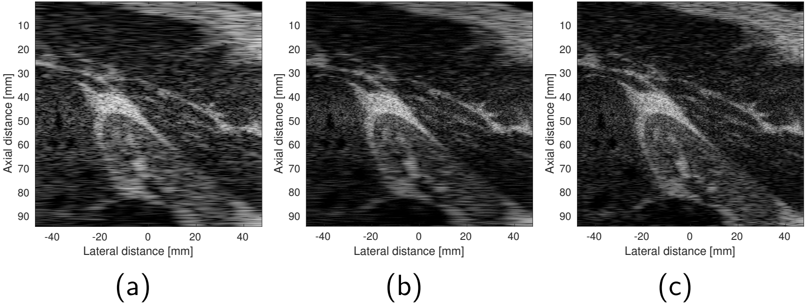

Figure : (a) Observed B-mode image simulated following the proposed axially-variant convolution model; (b) Spatially-invariant deconvolution result (in B-mode) obtained with a fixed kernel equal to $\mathbf{k}(m_t/2)$; (c) Spatially-variant deconvolution result (in B-mode) using our axially varying kernel mode;

Simulation: convergence rate

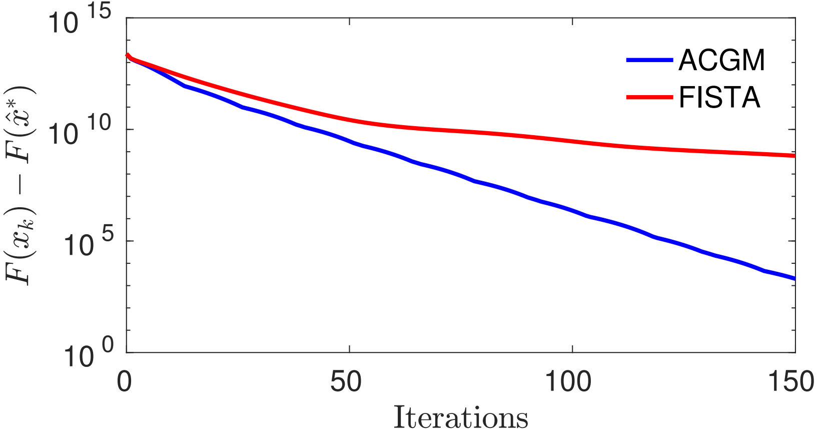

Figure : Convergence rate of our method compared to FISTA.

Additional reading

- Mihai I. Florea and Sergiy A. Vorobyov, "An accelerated composite gradient method for large-scale composite objective problems", *arXiv preprint* arXiv:1612.02352 [math.OC], Dec. 2016, under review at IEEE Transactions on Signal Processing.
- Mihai I. Florea and Sergiy A. Vorobyov, "A generalized accelerated composite gradient method: uniting Nesterov's fast gradient method and FISTA", *arXiv preprint* arXiv:1705.10266 [math.OC], May. 2017, under review at Journal of Optimization Theory and Applications.
- Mihai I. Florea, Adrian Basarab, Denis Kouamé, and Sergiy A. Vorobyov, "An axially-variant kernel imaging model for ultrasound image reconstruction", IEEE Signal Processing Letters (accepted), DOI: 10.1109/LSP.2018.2824764, 2018.
- Mihai I. Florea, Adrian Basarab, Denis Kouamé, and Sergiy A. Vorobyov, "An axially-variant kernel imaging model applied to ultrasound image reconstruction", *arXiv preprint* arXiv:1801.08479 [eess.SP], Jan. 2018.

Backup slides

Padding

- Allows us to reconstruct a TRF of the same size as the observed RF image
- Is an estimation of the surrounding tissues using information from the imaged TRF
- If this border information is not required, the reconstructed TRF can simply be cropped accordingly.

Computationally efficient padding

- Operator $\mathbf{P}$ is linear and separable along the dimensions of the image $\mathbf{P} = \mathbf{P}_m \mathbf{P}_n$.
- $\mathbf{P}_m$ pads every column of the image independently by applying the 1D padding (linear) operator $\mathscr{P}(m_t, m_r)$.
- The row component $\mathbf{P}_n$ treats every row as a column vector, applies $\mathscr{P}(n_t, n_r)$ to it, and turns the result back into a row.

Computationally efficient padding

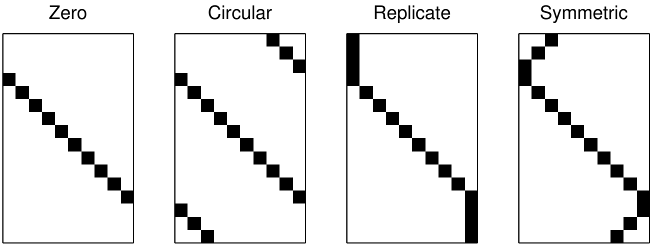

Figure : Common matrix forms of 1D padding operators $\mathscr{P}(10, 3)$. Black denotes a value of 1 and white denotes 0.

Theorem

Padding operator $\mathbf{P}$ *can be obtained programatically in the form of a sparse matrix as*

$$\mathbf{P} = \mathscr{P}(n_t, n_r) \otimes \mathscr{P}(m_t, m_r).$$

Notation: discrete convolution (analytical expression)

$$\mathbf{k} \in \mathbb{R}^{m_k \times n_k}, \quad m_a \geq m_k, n_a \geq n_k, \quad \mathbf{a} \in \mathbb{R}^{m_a \times n_a}$$

Valid convolution

$$(\mathbf{k} *_1 \mathbf{a})_{i,j} \stackrel{\text{def}}{=} \sum_{p=1}^{m_k} \sum_{q=1}^{n_k} \mathbf{k}_{p,q} \mathbf{a}_{i-p+m_k, j-q+n_k},$$

$$i \in \{1, \ldots, m_a - m_k + 1\},\ j \in \{1, \ldots, n_a - n_k + 1\},$$

Full convolution

$$(\mathbf{k} *_2 \mathbf{a})_{i,j} \stackrel{\text{def}}{=} \sum_{p=p_i}^{\bar{p}_i} \sum_{q=q_j}^{\bar{q}_j} \mathbf{k}_{p,q} \mathbf{a}_{i-p+1, j-q+1},$$

$$i \in \{1, \ldots, m_a + n_k - 1\},\ j \in \{1, \ldots, n_a + n_k - 1\},$$

$$p_i = \max\{1, i - m_a + 1\}, \quad \bar{p}_i = \min\{i, m_k\},$$

$$q_j = \max\{1, j - n_a + 1\}, \quad \bar{q}_j = \min\{j, n_k\}.$$

Notation: auxiliary operators (analytical expression)

Rotation operator

$$(\mathscr{R}(\mathbf{k}))_{i,j} \stackrel{\text{def}}{=} \mathbf{k}_{m_k-i+1,n_k-j+1},$$
$$i \in \{1,\ldots,m_k\}, \quad j \in \{1,\ldots,n_k\}.$$

Exception index set

$$\mathscr{I}(a,b,c) \stackrel{\text{def}}{=} \{1,\ldots,c\} \setminus \{a,\ldots,b\}, \quad 1 \le a \le b \le c$$

Full-width window and zero padding operators

$$(\mathscr{W}_s(i_1,i_2)\mathbf{a})_{i,j} \stackrel{\text{def}}{=} \mathbf{a}_{i+i_1,j}, \quad i \in \{0,\ldots,i_2-i_1\},$$
$$(\mathscr{Z}_s(i_1,i_2)\mathbf{a})_{i,j} \stackrel{\text{def}}{=} \begin{cases} \mathbf{a}_{i-i_1,j}, & i \in \{i_1,\ldots,i_2\}, \\ 0, & i \in \mathscr{I}(i_1,i_2,m_s), \end{cases}$$

where $j \in \{1,\ldots,n_s\}$ and index $s \in \{t,p\}$ stands for image size quantities m_t, m_p, n_t, and n_p.